

Monte-Carlo based Reduction of Motion in Contrast Agent enhanced MR-Mammographies

F. Hess¹, D. Krechel¹, L. Nakashima², A. v.Wangenheim²

Introduction

We present an algorithm for fast reduction of motion artifacts in MR images (MRI). The application field in the center of interest is the automatic detection of malignant tissue in contrast agent enhanced MR-Mammographies. Here, a series of up to ten MRI-volumes recorded at discrete time points is taken, describing the signal increase in tissue voxels (volume elements) by contrast agent enhancement (Gd-DTPA). Due to the patient's breathing, motion is induced and by this a dislocation of tissue areas over time. However, critical for a proper tissue classification is that the investigated tissue areas lie as accurately as possible at the same voxel positions of every acquired MRI-volume. Only by this, the signal behaviour of the tissue can be traced properly. Although signal averaging by windowing filters like 2D-Gaussian filters can reduce classification errors induced by tissue dislocation, the applied window size is limited by the given minimum size of tissue to be classified. In other words, applying a 17 square voxel window for the classification of 2 square voxel sized tissue structures is inadequate. A motion reduction technique between voxels of different MRI-volumes is necessary.

Our first approach towards motion reduction implemented in the MAMMA-LYZER-system [4] makes use of modified Kohonen maps as described in [7]. However, this method does not meet the time constraints set by our medical partners (Dr. Buddenbrock, Dr. Blasinger, Dr. Benz, Clinic for Radiology, Mainz, Germany) i.e. real-time applicability). This leads to the current approach as described in the following section.

Materials and Methods

MRI-volumes concerned here consist of 16 axial slices of the female mamma with slice dimensions of 256 x 256 voxels. The voxels themselves represent physical areas the size of 1x1x6 mm. As motion is mainly induced by the patient's breathing, the applied axial registration has the advantage that breathing takes places almost inside volume slices and not between them. This motivates a faster two dimensional motion reduction algorithm. Breathing results in coarse-scale and mainly linear motion, so it is feasible to determine voxel dislocations (disparities) at only a few tissue voxel positions serving as supporting points for a following interpolation of the remaining tissue voxels.

The actual calculation of voxel dislocations between two MRI-volumes (volume matching) makes use of a least square error based steepest gradient search followed by a Voronoi

¹ Arbeitsgruppe Expertensysteme/Künstliche Intelligenz, Universität Kaiserslautern, Postfach 3049, 67653 Kaiserslautern, Email: {hess,krechel}@informatik.uni-kl.de

² Department of Computer Sciences, Universidade Federal de Santa Catarina, 88049-900 Florianopolis - S.C., Brazil, Email: {nakashima,awangenh}@inf.ufsc.br

based disparity interpolation. The motion reduction process described here compares two MRI-slices P_1 and P_2 of two measured MRI-volumes V_1 and V_2 . For every voxel $p_{xy} := (x, y)$ of slices $P_1 := \{(x, y) \mid x \in \mathcal{N}, y \in \mathcal{N}\}$, it is necessary to determine the corresponding voxel $p_{x'y'}$ in slice P_2 . As consequence, the set $M := \{D_{xy} := (d_x(x, y), d_y(x, y)) \mid (x, y) \in P_1\}$, denoted as motion map, delivers for every voxel $p_{xy} \in P_1$ the disparity D_{xy} towards slices P_2 , if $d_x(x, y) = (x - x')$ and $d_y(x, y) = (y - y')$ holds for every corresponding voxel pair $p_{xy} \in P_1$ and $p_{x'y'} \in P_2$.

Speaking of voxel intensities $I_p(x, y)$ of voxel $p_{xy} \in P$, one can derive a matched slice $R := P_1$ out of P_2 for every voxel $p_{xy} \in P_1$ by means of

$$I_R(x, y) := I_{P_2}(x + d_x(x, y), y + d_y(x, y)), \quad (d_x(x, y), d_y(x, y)) \in M \quad (1)$$

By this, $I_R(x, y)$ denotes the proper voxel intensity of voxel $p_{xy} \in R$. Now, the correspondence problem reduces to finding the motion map M and therefore determining the disparity D_{xy} of every voxel in P_1 . Our approach makes use of the last square error calculation of voxel windows in P_1 and P_2 . Given a voxel $p_{xy} \in P_1$ to be further investigated, the native window in P_1 having a certain size is centered at p_{xy} while the test window in P_2 of the same size is moved around p_{xy} . Looking at the square error calculation of both windows (see equation 2), a least square error occurs where both windows fit best with respect to their voxel intensities.

Given a native window $NW := \{(x', y') \mid x' \in [x - c_x; x + c_x], y' \in [y - c_y; y + c_y]\}$ and an error window $EW := \{(x', y') \mid x' \in [-e_x; e_x], y' \in [-e_y; e_y]\}$ with width and heights c_x, c_y, e_x and e_y , one can derive the least square error disparity $D_{xy} = (d_x(x, y), d_y(x, y))$ of voxel p_{xy} by

$$D_{xy} = \arg \min_{(x', y') \in CW} \sqrt{\sum_{(x'', y'') \in EW} (I_{P_1}(x + x'', y + y'') - I_{P_2}(x' + x'', y' + y''))^2} \quad (2)$$

It is in terms of computational efforts suitable to apply a Monte-Carlo based method for determining M . This means, only a fraction of voxels $p_{xy} \in P_1$ containing tissue information is processed in the above described way, and those remaining gain their disparity D_{xy} by an interpolation process.

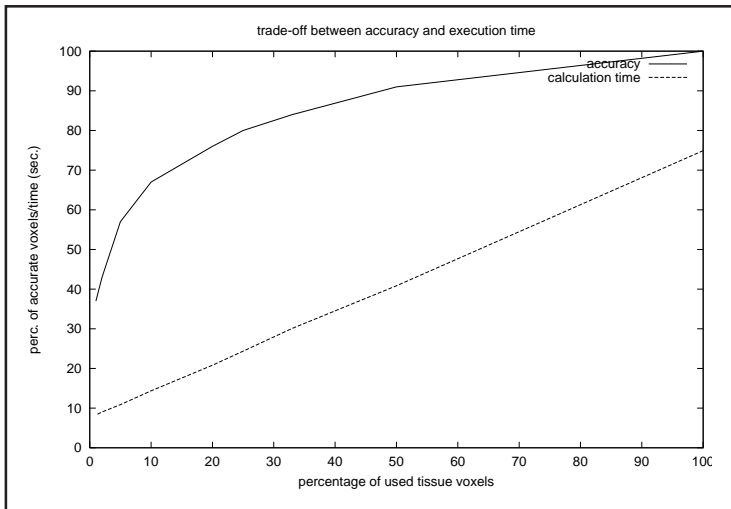


Fig. 2: Trade-off between calculation accuracy and calculation time. Although the calculation time develops linearly with the amount of supporting points, the calculation accuracy (i.e. the percentage of correctly matched voxels) decreases dramatically when using less than 10 percent of possible supporting points. Note that the fixed calculation time of about 8 secs. is due to image reading and storing processes.

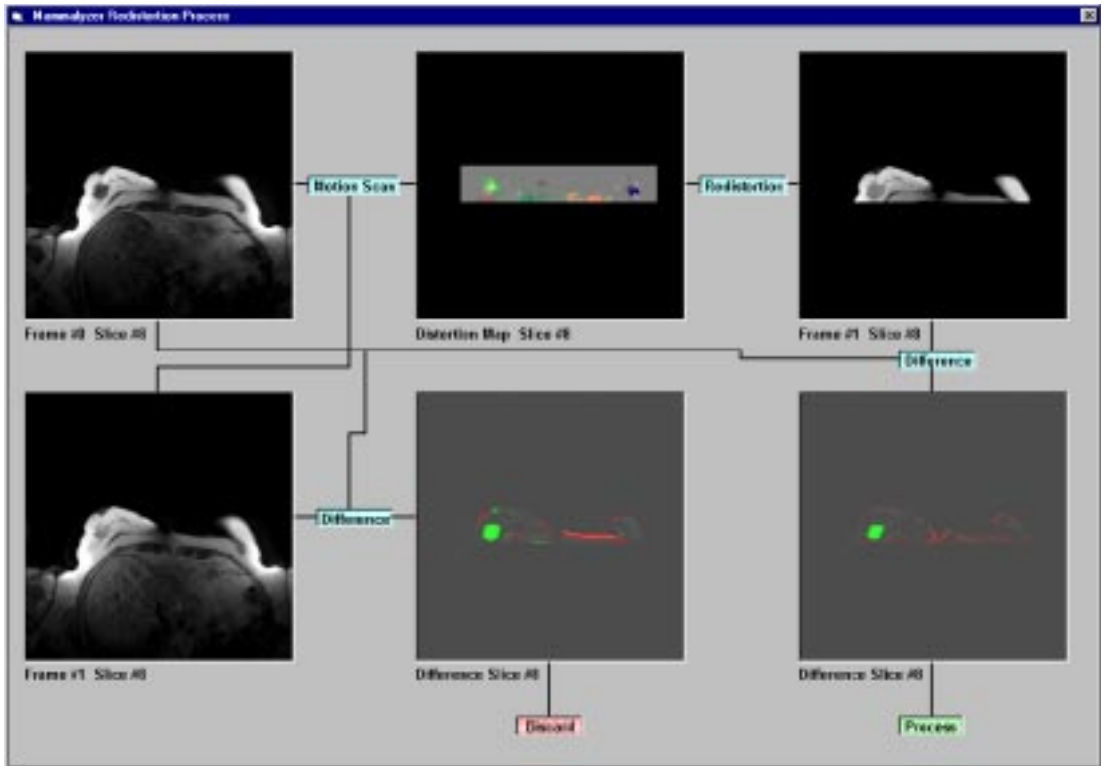


Fig. 1: Motion artifact reduction process. Using a least square error approach, two slices of different MRI-volumes (upper and lower left) are matched by creating a motion map (upper middle) and by relocating voxel intensities (upper right). The matching results are shown as difference pictures between both source images (lower middle) and between the source native slice (upper left) and the resulting matched slice (upper right). As can be seen, motion artifacts are reduced, although a contrast agent enhancement has taken place.

Results and Discussion

Fig. 1 shows the whole motion reduction process as described before. Due to the Monte-Carlo-based approach interpolation errors can occur when determining the slice's motion map. This results in an erroneous voxel matching process. Fig. 1 shows the impact of supporting points used for the interpolation on the amount of wrongly matched voxels. Here, an averaging window (Gaussian, std. dev. = 2 voxels) is already applied. As can be seen, there is a trade-off between the accuracy of matching and its calculation time.

Currently, our efforts focus on a validation of the developed algorithms with data supplied by our medical partners, a hardware implementation using FPGAs (field programmable gate arrays), and an application to MR head images.

References

1. Heywang-Köbrunner, S.: Contrast- Enhanced MRI of the Breast. Basel: Karger/ Schering 1990.
2. Kaiser; Werner; Diedrich; Reiser; Krebs: Moderne Diagnostik der Mamma. Geburts- u. Frauenheilkunde 1993.
3. Makabe, M.; Glomitz, G.; Mayer, A.; Meinzer, H. P.; Lederer, W.; Schneider, S.; Wrazidlo,

- W.: Interpretation Support of Contrast-Enhanced MR-Mammography by Image Processing. CAR 1995.
4. Huwer S.; v.Wangenheim, A.: MAMMALYZER: An Approach for Automatic Detection of Breast Cancer by Analyzing Contrast-Enhanced MRI-Mammographs. AIM- 96 - Symposium on Artificial Intelligence in Medicine, Stanford 1996.
5. v. Wangenheim, A.: Cyclops: Ein Konfigurationsansatz zur Integration hybrider Systeme am Beispiel der Bildauswertung. Diss.; Universität Kaiserslautern 1996.
6. Kelcz, F.; Giles, E.; Santry, C. G.; Mongin, S.: Application of a Quantitative Model to Differentiate Benign from Malignant Breast Lesions Detected by Dynamic, Gd-enhanced MRI. JMRI September/October 1996.
7. Huwer, S.; Rahmel, J.; v.Wangenheim, A.: Data-Driven Registration for Local Deformations. Pattern Recognition Letters. North-Holland 1995.
8. Comes, R.: Konzeption und Implementierung einer bildauswertungsorientierten Konfigurationswissensbasis. Diplomarbeit, Universität Kaiserslautern 1997.
9. Haralick, R. M.; Shapiro, L.: Computer and Robot Vision II. Addison Wesley 1993.
10. Goshtasby, A.; Turner, D.; Ackerman, L.: Matching of tomographic slices for interpolation. IEEE Transact. on Med. Imag. 11, 1992.